ELSEVIER

Structure and electrochemical properties of Ti$_{0.25}$V$_{0.35}$Cr$_{0.40-x}$Ni$_x$ ($x = 0.05$–0.40) solid solution alloys

Yujun Chai, Minshou Zhao*

Key Laboratory of Rare Earth Chemistry and Physics, Changchun Institute of Applied Chemistry, Chinese Academic of Science, Changchun 130022, China

Abstract

The structure and electrochemical properties of Ti$_{0.25}$V$_{0.35}$Cr$_{0.40-x}$Ni$_x$ ($x = 0.05$–0.40) solid solution alloys have been studied in the paper. It is found that these alloys consist of a main solid solution phase with body centered cubic (bcc) structure and a little TiNi-based secondary phase. The solid solution alloys show easier activation behavior at 313 K as a negative electrode material for MH–Ni battery. With changing x from 0.05 to 0.30, the discharge capacity and the high-rate dischargeability increase. The discharge capacity increases with increasing temperature. The maximum discharge capacity is 240 mA h/g at 313 K for $x = 0.30$ and 280 mA h/g at 343 K for $x = 0.15$.

1. Introduction

Nickel–metal hydride battery has attracted more attention than Ni–Cd battery due to its high-energy density, long cycle life, high-rate capability and its cleanliness. Among hydrogen storage alloys, solid solution alloy with body-centered cubic (bcc) structure, such as V and V-based alloy, can reversibly absorb/desorb more amount of hydrogen, and some papers are published on this topic [1,2]. The negative electrode materials in nickel–metal hydride battery, which contain solid solution alloy, essentially include V$_3$TiNi$_{0.56}$, TiV$_{2.1}$Ni$_{0.3}$ and non-stoichiometric AB$_2$-type alloys (Ti-based). In general, the solid solution alloy works as a hydrogen storage medium, and C14 Laves phase or TiNi-based second phase acts as a micro-current collector or electrocatalyst, and then improves the electrochemical property of alloy electrodes [3–6]. Ti–V-based solid solution alloy, which has a high effective hydrogen storage capacity, has recently been presented by Akiba [7,8].

It has been pointed out that the alloy of Ti$_{0.25}$V$_{0.35}$Cr$_{0.40}$ with bcc structure has a high effective hydrogen storage capacity, and the highest is 2.2 mass% at 313 K. Iba further reported that the addition of Ni from 0.05 to 0.15 could remarkably improve the discharge capacity [9]. However, the effect of Ni on the electrochemical property of the solid solution alloy has not yet been systematically reported. In this paper, the structure and electrochemical properties of Ti$_{0.25}$V$_{0.35}$Cr$_{0.40-x}$Ni$_x$ ($x = 0.05$–0.40) solid solution alloys are relatively discussed in detail.

2. Experimental

Samples of Ti$_{0.25}$V$_{0.35}$Cr$_{0.40-x}$Ni$_x$ ($x = 0.05$–0.40) alloys were melted by arc melting under an argon atmosphere. In order to get a homogeneous alloy, the alloy ingots were turned over and remelted at least four times. Then the as-cast alloys were crushed mechanically in air and further pulverized with a ceramic mortar to the project supported by powder of 200 meshes. The electrodes were prepared by mixing the alloy powder with porous nickel powder in a weight ratio of 1:5, and then cold pressing the mixture to

---

* Corresponding author. Fax: +86-431-5262365.
 E-mail address: zhaoms@ciac.jl.cn (M. Zhao).

form pellets. Prior to electrochemical testing, all alloy electrodes were activated by immersion in 6 M KOH aqueous solution for 2 days. The positive electrode was a sintered $Ni(OH)_2/NiOOH$ plate. The charge/discharge tests were carried out by DC-5 battery testing instrument with computer control. The alloy electrodes were charged with a current density of 60 mA/g or discharged with a current density of 60 mA/g to the cut-off voltage of 0.8 V in a water-bath.

In order to evaluate the crystal structure, XRD analysis of $Ti_{0.25}V_{0.35}Cr_{0.40-x}Ni_x$ alloys was carried out on a RIGAKU D/max-II B X-ray diffractometer using Cu Kα radiation at 40 KV and 200 mA. The microstructure of the solid solution alloy and composition of each phase were determined by scanning electron microscopy and energy dispersion X-ray spectroscopy.

3. Result and discussion

3.1. Alloy structure

The typical X-ray diffraction patterns are shown in Fig. 1. It can be seen that the alloys are composed of a main phase with a bcc structure and a little TiNi-based secondary phase determined by energy dispersion X-ray spectroscopy. With changing x, from 0.05 to 0.40, the substitution of Ni for Cr makes the main peak position to gradually shift to a higher angle direction, which implies that the increase in x leads to lattice parameter shrinkage. The calculated lattice parameter of solid solution changes from 3.010 to 2.987 Å as shown in Table 1. When $x = 0.40$, more peaks appear and the microstructure of the alloy would change.

Fig. 2 gives the scanning electron micrographs of $Ti_{0.25}V_{0.35}Cr_{0.40-x}Ni_x$ ($x = 0.05$–0.40) solid solution alloys.
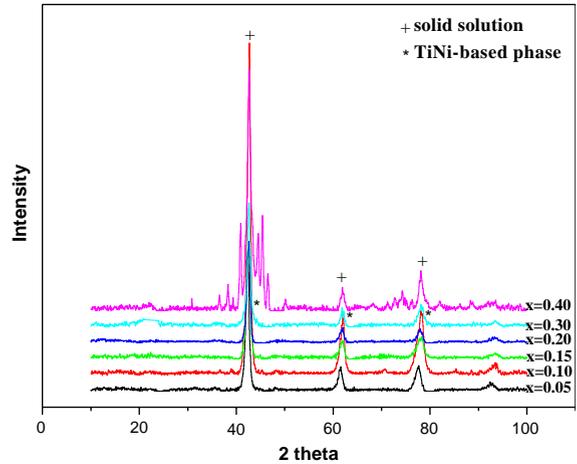

Fig. 1. XRD patterns for $Ti_{0.25}V_{0.35}Cr_{0.40-x}Ni_x$ ($x = 0.05$–0.40) alloys.

From the graphs, it can be seen that with increasing Ni the secondary phase increases and further increasing secondary phase aggregates at grain boundary, encircles the solid solution, and finally forms the network structure. The composition of the solid solution and TiNi-based secondary phase is examined semi-quantitatively by energy dispersion X-ray spectroscopy. The results are listed in Table 1. With increasing Ni content, Ti content decreases and V content increases in solid solution phase. However, Cr content decreases and Ni content increases in both solid solution and TiNi-based secondary phase. The results indicate that V mainly exists in the solid solution, and a large amount of Ti precipitates with the element Ni along grain boundary as imaged by SEM, which agrees well with the result presented by Tsukahara [3].

Table 1
Composition and structure of $Ti_{0.25}V_{0.35}Cr_{0.40-x}Ni_x$ ($x = 0.05$–0.40) alloys

x	Phase	Composition(atom %)				Lattice parameter (Å)	Cell volume (Å)
		Ti	V	Cr	Ni		
0.05	bcc	17.19	42.37	38.16	1.83	3.010	27.27
	Secondary phase	17.69	58.42	22.21	1.68		
0.10	bcc	16.51	44.05	36.84	2.59	2.989	26.70
	Secondary phase	27.42	49.97	20.79	1.83		
0.15	bcc	12.78	48.81	35.46	2.95	2.989	26.70
	Secondary phase	31.11	45.72	20.22	2.95		
0.20	bcc	11.1	58.9	24.22	5.78	2.988	26.68
	Secondary phase	35.34	40.57	7.34	16.75		
0.30	bcc	11.43	62.82	15.19	10.55	2.986	26.62
	Secondary phase	38.5	25.13	3.58	32.79		
0.40	bcc	7.81	67.51	—	24.68	2.987	26.65
	Secondary phase	21.73	38.71	—	39.56		